KSME

Springer

Journal of Mechanical Science and Technology 34 (11) 2020

Original Article
DOI 10.1007/s12206-020-10 -y

Keywords:
· Solar energy
· Fresnel collector
· Cylindrical-parabolic collector
· Steam
· Hot water

Correspondence to:
Cuma Çetiner
ccetiner@gmail.com

Citation:
Çetiner, C. (2020). Experimental and theoretical analyses of a double-cylindrical trough solar concentrator. Journal of Mechanical Science and Technology 34 (11) (2020) ?~?. http://doi.org/10.1007/s12206-020-09 -y

Received ?? th, 2020
Revised ?? th, 2020
Accepted ?? th, 2020

† Recommended by Editor ??

Experimental and theoretical analyses of a double-cylindrical trough solar concentrator

Cuma Çetiner

Department of Mechanical Engineering, Faculty of Engineering, Harran University, Şanlıurfa, Turkey

Abstract Parabolic trough, Fresnel, heliostat mirror, or dish-type collectors are used to obtain high temperature in solar thermal applications. The operation of this system is similar to that of a Fresnel collector, except for its reflective mirror, which is cylindrical and not flat. The experiments were carried out in the solar energy system manufactured for producing hot water, superheated water, and steam in the cylindrical trough solar concentrator. According to the test results, the thermal power of the system and the average thermal efficiency of the collector were a maximum of 15 kW and approximately 35 %, respectively.

1. Introduction

Studies on solar energy applications and technologies have been increasing rapidly in recent years. The use of flat-plate type collectors is enough to meet the demand for hot water, which is a type of solar energy with low thermal temperature [1, 2]. However, the use of concentrating collectors is necessary for high-temperature applications obtained from solar energy in the industry [3, 4]. Parabolic trough collector system, linear Fresnel collector (LFC), central tower concentrating solar power, and parabolic dish concentrator are used in high-temperature applications. These collectors collect the sun's rays in a linear or point focus. The temperature can be increased to up to 150 °C-500 °C in linear concentration [5-7] and 1400 °C in point concentration in focusing collectors depending on their geometric shapes [8, 9]. Central-receiver and dish collectors are used at high-temperature applications. Parabolic trough and LFC are used on commercial and industrial scales for medium-temperature applications [10].

Fresnel collectors are used for focusing on solar radiation through a series of flat, long, and parallel mirrors. The rays reflected from the flat mirrors are transferred to the liquid that circulates in the absorber in the focus of the system. The receiver in the focus of the Fresnel collectors is a flat or a compound absorber that reflects radiation the second time [11, 12]. With LFC, many studies, including the LFC prototype made by Solarmundo in Belgium, have been conducted worldwide to achieve high temperatures [13]. Plataforma Solar de Almeria worked on prototype projects to achieve 400 °C temperature with LFC in Spain and Italy. Novatec Solar, Areva Solar, and SkyFuel companies have carried out important works to develop linear Fresnel technology [10, 14]. To improve the performance of LFC, many studies are carried out on the flat collector and compound absorber [15-19].

A linear receiver is found in the middle of the LFC. Flat mirrors with solar tracking systems reflect their radiation to this receiver. The mirror can bend at a certain rate and this mirror feature has been used in this study. A cylindrical surface can be obtained for ease of manufacture and economy. Studies in this field are found in the literature. Nicolas [20] carried out and compared the mathematical analyses and designs of cylindrical-parabolic and fixed-reflector linear focusing and fixed-surface concentrators according to the methods of tracking sun rays. Kulkarni [21] designed a cylindrical parabolic collector, which had an aperture area of 1.89 m^2 and reached 69 % thermal efficiency for 60 ^{o}nce. Sadhana [22] carried out a theoretical study for the design of a cylindrical parabolic collector for 125 ^{c}ow needed for the sterilization of medical devices

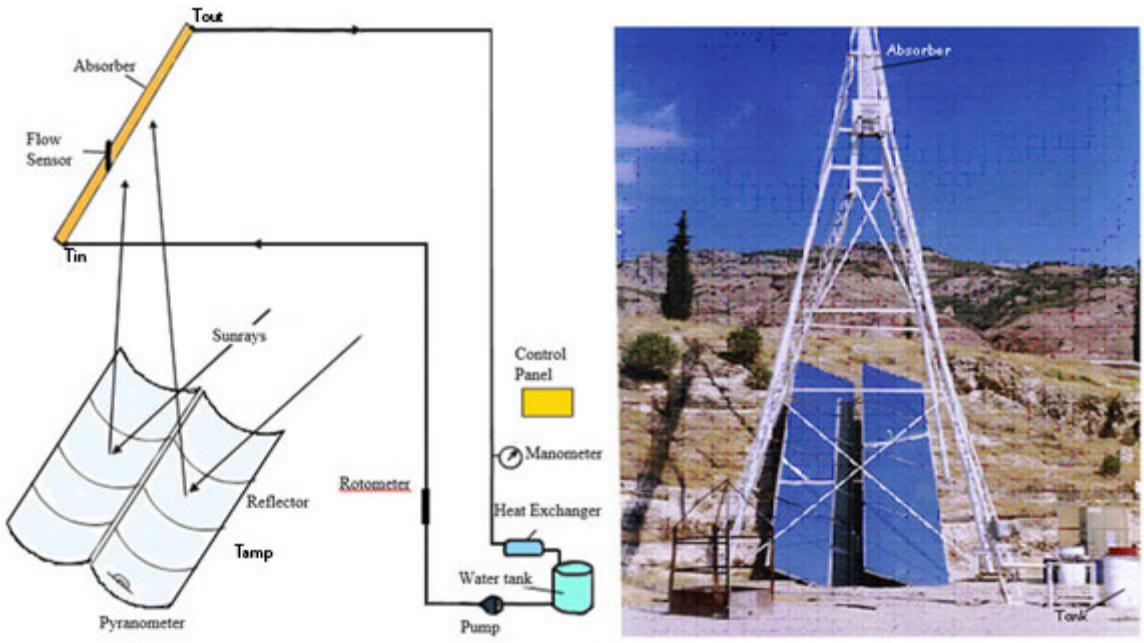

Fig. 1. Experimental set up of fixed-concentrating double-cylindrical trough solar concentrators.

according to the radiation values of the region. As parabolic concentrators operate according to the reflection method, they must own a solar tracking system. Preveen [23] determined that the efficiency of the fixed-axis was 12 % and the efficiency of the system with solar tracking was 19 % based on his study on the performance of fixed collectors and collectors with a solar tracking system.

Most of the studies that concentrate on solar energy, parabolic reflector, and absorber track the sun together [24]. In this study, cylindrical reflective mirrors, which are similar to Fresnel collector types, track the sun, and their focus (absorber surface) stays fixed. If the focus is not fixed, then the tracking the sun together with focus in large systems results in various mechanical problems in the entire system in terms of construction. Moreover, the heat-transferring pipes connected to the absorber must be moving. Fresnel-type collectors are usually placed on the horizontal axis. However, this set of experiments was placed on the same slope as the 37° latitude of the region. This type of settlement is called the polar axis. Polar-traced collectors can work efficiently at high temperatures.

2. Experimental setup

As shown in Fig. 1, the experimental setup consists of two cylindrical trough-type reflective mirrors, a absorber surface, a pump, a heat exchanger, a sun-tracking mechanism, a flow sensor, a water tank, a pyranometer, temperature, pressure, and flow meters. Each cylindrical reflector consists of a 27 m^2 mirror. The total area of the reflective mirrors in two cylindrical troughs is 54 m^2. The focal length is 12 m.

Therefore, the ratio of the focal length to the linear semi-aperture is 5.7. This value shows that the cylindrical mirror is almost linear. This phenomenon is called the paraxial region, and the cylindrical surface can be accepted as a parabola in the paraxial region. Thus, two 2.1 m-wide cylindrical reflectors were used instead of a 4.2 m-wide single-cylindrical reflector.

In this study, two Kipp-Zonen CM11 pyranometers were used to measure solar radiation diffusion. The inlet and outlet temperatures of the water in the absorber surface were measured using Fe-Co J-type thermocouple, and inlet and outlet pressures were measured using a manometer. Pure water was used in the setup. In the experiments conducted for steam, the flow sensor was placed in the absorber to control the water level. The flow sensor operates the water pump when the water level decreases and stops the water pump when the water level increases. During the experiments, the measurements were taken every 15 minutes starting at 9:00 in the morning and ending at 17:00.

3. Theoretical analysis

Although some of the solar radiation energy that reaches the absorber from the concentrator is emitted to the environment with a lower temperature through transmission, convection, and thermal radiation, the other part is absorbed by fluid and turns into useful energy. The heat losses in the absorber are realized through conduction, convection, radiation from the glass cover, and insulation to the environment. The absorber used in this experimental setup has a flat absorber, and a flat glass was placed on its front surface. A 50 cm-thick thermal insulation was installed on the rear surface as protection from the external environment. In Fig. 2, the shape of the absorber looks similar to a flat collector. Therefore, the calculation used for flat collectors can also be used here with consideration to

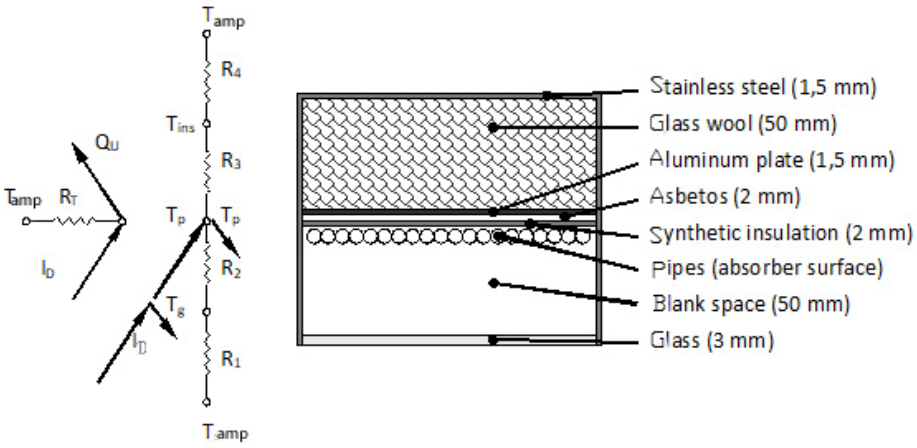

Fig. 2. Thermal resistances in the absorber according to the electrical analogy method.

the concentration.

The Hottel-Whiller-Bliss equation, which is the most widely used equation for finding useful energy in flat collectors, can also be used for concentrating collectors [25]. As such, for useful energy gain, the following equation can be written.

$$Q_u = A_a F_R \left[I_a - \frac{A_c}{A_a} U_T \left(T_{in} - T_{amb} \right) \right], \quad (1)$$

where Q_u is the useful energy, A_c is the total aperture area, A_a is the absorber area, F_R is the heat gain factor, T_{in} is the fluid inlet temperature, T_{amp} is the ambient temperature, I_a is the intensity of direct solar radiation that comes to the absorber surface, and U_T is the total heat transfer coefficient. The intensity of direct solar radiation coming to the absorber surface is [26]:

$$I_a = (\tau\alpha)\gamma\rho I_d, \quad (2)$$

where I_d is the amount of direct radiation coming on the unit aperture area, γ the intercept factor, τ is the radiation transmission coefficient of the transparent cover, α is the ratio of absorbing radiation of the absorber material, and ρ is the ratio of the reflection of the reflective mirror. The collector thermal efficiency is [25].

$$\eta = \frac{Q_u}{A_c I_d}. \quad (3)$$

The theoretical calculations of the thermal power and thermal efficiency of this system have been published in another publication (30).

4. Thermal losses in the absorber surface

Thermal losses in the absorber were calculated as follows [27, 28].

$$Q_{loss} = \frac{\left(T_P - T_{amb} \right)}{R_T} = U_T A_c \left(T_p - T_{amb} \right), \quad (4)$$

where T_p is the absorber surface temperature, T_{amb} is the ambient temperature, R_T is the total thermal resistance, U_T is the total heat loss coefficient, and A_c is the surface area of the absorber. Total thermal resistances are depicted in Fig. 2. The total thermal resistance (R_T), is equal to the sum of convection thermal resistance between the external environment and the glass cover at the bottom (R_1), the thermal resistance of the air gap between the glass cover and the absorber (R_2), the thermal resistance of the insulation layer (R_3), and convection thermal resistances between the upper part of the absorber, and the external environment (R_4). For the total heat loss coefficient in the absorber, thermal losses from the lower, upper, and side surfaces of the absorber must be determined. In the lower part of the absorber, the total heat loss coefficient between the absorber surface and the environment is expressed as follows (29):

$$U_{und} = \frac{1}{R_1 + R_2}, \quad (5)$$

$$U_{upper} = \frac{1}{R_3 + R_4}, \quad (6)$$

$$U_{sur} = 0,6 \left[\frac{A_{a-sur}}{A_a} \right], \quad (7)$$

$$U_T = U_{und} + U_{upper} + U_{sur}, \quad (8)$$

where U_{und}, U_{upper}, and U_{sur} are the heat transfer coefficient of the lower part, upper part, and side of the absorber, respectively. The equations used to determine the total heat transfer coefficient are given in detail in the publication [30].

5. Experimental results and discussion

In this test set, three kinds of experiments were performed at

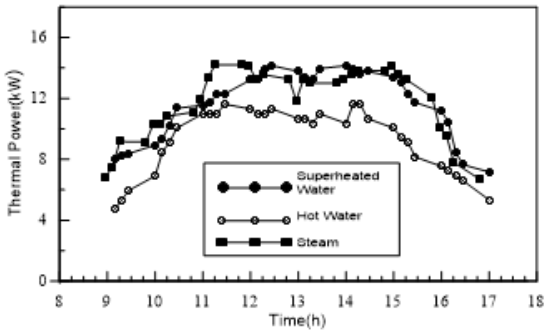

Fig. 3. Comparison of the thermal powers in the experiments conducted using hot water, superheated water, and steam.

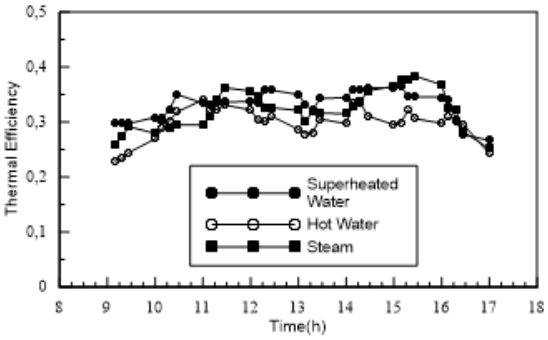

Fig. 4. Comparison of the collector efficiencies in the experiments conducted using hot water, superheated water, and steam.

different flow rates and pressures: "steam," "super-heated water" refers to the water under pressure at temperatures above 100 °C and is also known as "pressurized hot water," and at the atmospheric pressure "hot water." Experiments were conducted in Denizli-Kızıldere (Lat. 37.1) and from 9:00 a.m. in the morning to 17:00 p.m. in the afternoon.

In the experiment conducted for steam generation at 3 bars pressure, the minimum and maximum flow rates were 12 lt/h and 19 lt/h, respectively. The ambient temperature varied between 18 °C-26 °C. The outlet temperature of the steam from the absorber was adjusted to be continuously higher than 133 °C (137 °C-138 °C), which is the saturated water temperature for the 3 bars pressure.

The superheated water experiment was conducted at a flow rate of 160 lt/h and 2.2 bars pressure. On the day of the experiment, the direct solar radiation began from 550 W/m^2, reached 830 W/m^2, and decreased to 550 W/m^2 at the end of the experiment. The ambient temperature varied between 22 °C-31 °C on the day of the experiment. Fluid inlet temperature ranged from 54 °C-63 °C. and outlet temperature ranged from 97 °C-124 °C.

In the hot water experiment performed at the flow rate of 270 lt/h, the inlet temperature was between 40 °C and 60 °C, and the outlet temperature was between 60 °C and 95 °C. On the day of the experiment, direct solar radiation intensity varied between 450 W/m^2 and 750 W/m^2 during the day, and the ambient temperature varied between 21 °C and 32 °C from the morning to the evening. The measured temperature values for all three experiments are indicated in Table 1.

In the experiments with steam, superheated water, and hot water, the thermal power obtained from the system ranged from 4 kW to 15 kW, and the thermal efficiency ranged from 25 to 38. The flow rates of hot water, superheated water, and steam is 270 lt/h, 160 lt/h, and 19 lt/h, respectively. In this study, instead of comparing experimental values and theoretical calculations for each of the three experimental types, thermal efficiency, and thermal power of the experimental and theoretical results of hot water were compared.

To compare the results that were obtained by the theoretical calculation method with the results of the experiment, the theoretical calculation was made considering the conditions of the experiment that was conducted with hot water with the flow rate of 270 lt/h. In the theoretical calculation, the thermal efficiency and thermal power of the collector were calculated using the intensity of radiation measured at the time of the experiment. The comparison of the theoretical calculation and the experimental values for the hot water at a flow rate of 270 lt/h were given in Fig. 5. The thermal power found according to the theoretical calculation was approximately 5 % higher than the experimental values.

Theoretical and experimental collector efficiencies are presented in Fig. 6. The efficiency curve found by theoretical calculation was close to linear. The reason is because the factors that affect the theoretical calculation did not vary greatly, and the calculation was performed according to the net unshaded area in theoretical calculation. In the theoretical calculation, the collector efficiency did not very much in the morning, noon, and evening hours, and the efficiency was found to be approximately 35 %. The thermal efficiency was 28 %, 35 %, 28 %, and approximately 30 % in the morning hours, in the noon hours, in the evening hours, and the mean daily, respectively (Fig. 6).

Standard efficiency curves of solar collector systems, radiation intensity, windy environment, water inlet, and outlet and ambient temperatures vary. Therefore, the working point parameters of each collector may be different. Standard curves accepted by ASHRAE 93-77 were used to compare the experiments [26, 30]. In addition, the collector can be tested using different methods [18, 19, 34, 35].

The thermal efficiency Eq. (3), ambient and inlet temperature, and direct radiation values in Table 2 were used to determine the performance test values of the system. The regression analysis of (T_{in} -T_{amp} /I_d) (X) and the graph that corresponds to the thermal efficiency (Y) and working point parameter were created. Coefficients (a) and (b) were found in the correct equation. Hot water test regression analysis was performed, and the coefficients of the equation were (a) 0.34 and (b) −0.68, and nine equations were found [31, 32].

$$\eta_{th} = 0.34 - 0.68\left(\frac{T_{in} - T_{amp}}{I_d}\right) \quad (9)$$

Table 1. Temperature values of hot water, superheat water, and steam experiments.

	Hot water			Superheat water			Steam		
Time (h)	$T_{amp.}$ °C	T_{in} °C	T_{out} °C	$T_{amp.}$°C	T_{in} °C	T_{out} °C	$T_{amp.}$ °C	T_{in}°C	T_{out} °C
9:15	21	32	51	22	62	100	18	24	120
9:30	21,5	36	55	22,5	61	102	18	24	128
9:45	22	38	59	23	61	104	19	24	130
10:00	22,2	40	67	24	57	104	19	26	131
10:15	22,4	45	77	24,4	57	105	21	28	131
10:30	22,8	50	81	24,6	54	109	22	29	134
10:45	23	52	83	24,8	55	112	23	30	135
11:00	23,6	55	92	25	55	113	23,2	31	135
11:15	24	57	90	25,5	56	114	23,4	32	136
11:30	24,5	58	93	25,8	56	115	23,6	33	137
11:45	25	58	96	26	56	116	24	34	138
12:00	25,5	57	93	27	57	117	24	35	137
12:15	26,4	57	92	27,5	58	115	24,5	35	138
12:30	27,8	57	90	27,8	58	114	24,5	36	139
12:45	28,4	57	93	27,8	59	114	25	37	139
13:00	29	57	94	28	60	118	25	38	139
13:15	29,4	60	93	28,3	62	117	25	38	138
13:30	30	61	93	28,7	62	118	25	38	137
13:45	30,4	60	94	29	60	120	25	38	137
14:00	31	59	91	29	60	121	25	38	136
14:15	31,5	58	95	29,5	61	122	25	38	138
14:30	31,8	58	95	30	61	124	25	39	137
14:45	32	58	91	30,5	61	123	25	39	139
15:00	32,2	57	89	31	62	120	25	39	140
15:15	32	57	87	31	62	118	25	39	139
15:30	32	57	85	31	61	113	25	39	138
15:45	31,5	56	81	31	61	112	26	39	137
16:00	31	56	80	31	62	108	26	39	136
16:15	31	56	79	31	62	104	26	40	135
16:30	31	56	78	31	63	101	26	40	134
16:45	31	56	77	31	63	97	26	40	133
17:00	31	56	73	31	63	94	26	41	132

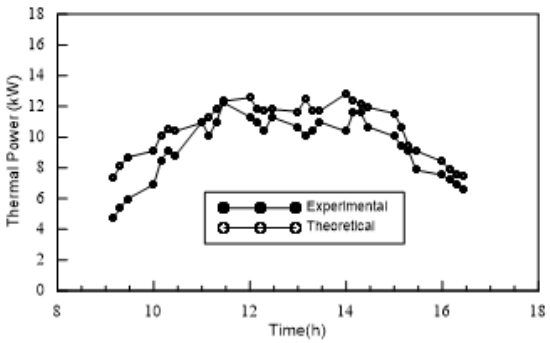

Fig. 5. Comparison of theoretical and experimental thermal powers for the case of hot water at the flow rate of 270 lt/h.

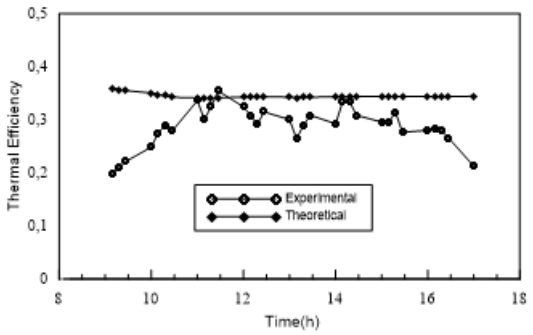

Fig. 6. Comparison of theoretical and experimental thermal efficiencies for the case of hot water at the flow rate of 270 lt/h.

Table 2. Hot water test values for regression.

Time (h)	T_{amp} °C	T_{in} °C	T_{out} °C	Direct Rad.W/m^2	$(T_{in}-T_{amp})/I_d$ m^{2}C/W	Thermal efficiency %
14:30	32	58	95	722	0,036	0,34
14:45	32,2	57	91	715	0,035	0,31
15:00	32	57	89	709	0,035	0,3
15:15	32	57	87	655	0,038	0,3
15:30	31,5	56	85	588	0,042	0,32
15:45	31	56	82	556	0,045	0,31
16:00	31	56	80	527	0,047	0,3
16:15	31	56	79	487	0,051	0,31
16:30	31	56	78	474	0,053	0,3
16:45	31	56	77	464	0,054	0,3
17:00	31	56	73	459	0,054	0,24

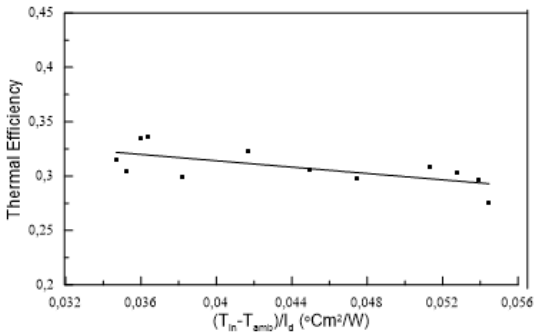

Fig. 7. Thermal efficiency of the collector for operation heat water.

In this graph (Fig. 7), the slope of the line shows a gradually decreasing structure. Although the efficiency of the system is low, it is compatible with the curves of such systems. Similar studies can be found in the literature. Singh [14], produced absorbers in four different designs with the Fresnel reflector. He found the equations of the thermal curves and showed them in graphs by determining the operating conditions of each absorber. Nayak [31] compared ASHRAE 93-863 standard with three different tests (e.g., Perers, DSc, and Wijeysundera) for flat collector. Amer [33] conducted a similar comparison study and compared ASHRAE 93-86 standard with other test methods (e.g., Saunier, Exell, Rogers, and filter method)

6. Conclusions

In the experiments conducted on the double-row cylindrical trough-shaped solar energy concentrator with an aperture area of 54 m^2, the thermal efficiency of the system varied between 23 % and 35 % during the day. A maximum of 15 kW thermal power was obtained from the system.

In the studies conducted using hot water, when the flow rate of water increased, approximately 5 % decrease was observed in the thermal efficiency and thermal power.

In the experiments performed for steam, the thermal efficiency of the system was approximately 35 % for the steam at 2, 3, and 4 bar pressures and approximately 30 % in the morning and evening hours. However, the system was investigated at a maximum temperature of 160 °C.

The theoretical and experimental thermal power values were very close to each other (Fig. 5). The efficiency curve found in consequence of the theoretical calculation was close to a straight line. The reason is that the factors affecting the theoretical calculation did not vary much and the calculation was performed according to the net unshaded area in the theoretical calculation (Fig. 6).

In calculating the experimental results, the thermal efficiency was calculated without removing the shaded areas to be realistic. The removal of the shaded areas provides an increased efficiency of approximately 10 %. This finding means that the shades should be minimized while designing the system.

Temperature of up to 150 °C can be used in desired practices industrially through this cylindrical system. The steam needed by some industrial enterprises can be obtained from the solar energy using this system, as well as in drying and heating systems. If the system is set up in wide areas in uncultivated land sloping areas, then it will not affect the agricultural regions negatively because of the ease of manufacturing when compared with the parabolic-surfaced collectors. If it is installed in a wider area, then electricity can be generated by collecting thermal energy at a center. Power plants might be established in wide areas because generating more steam with cylindrical trough-shaped solar energy systems is possible.

Nomenclature

Aa	: Absorber surface area (m^2)
Ac	: Total aperture area (m^2)
Cp	: Specific heat of fluid (kJ/kg K)
I_a	: Radiation coming to the absorbent surface (W/m^2)
I_d	: Direct radiation (W/m2)
$\dot{m}$	: Flow rate of the fluid (kg/s)
R	: Thermal resistance
T_{in}	: Water inlet temperature °C
T_{out}	: Water outlet temperature °C
T_p	: Absorber surface temperature °C
T_{amb}	: Ambient temperature °C
U_T	: Total heat transfer coefficient (W/m^{2}K)
Q_u	: Thermal power (kW)
F_R	: Heat gain factor
γ	: Intercept Factor (0.99)
η	: Collector thermal efficiency
τ	: Radiation transmission coefficient (0.88)
α	: The ratio of absorbing radiation (0.91)
ρ	: The ratio of reflection (0.83)

References

[1] M. Chekerovska and R. V. Filkoski, Efficiency of liquid flat-plate solar energy collector with solar tracking system, *Thermal Science*, 19 (5) (2015) 1673-1684.

[2] Y. W. Koholé and G. Tchuen, Experimental validation of exergy optimization of a flat-plate solar collector in a thermosyphon solar water heater, *Arabian Journal for Science and Engineering,* 44 (2019) 2535-2549.
[3] B. Evangelos and T. Christos, Alternative designs of parabolic trough solar collectors, *Progress in Energy and Combustion Science,* 71 (2019) 81-117.
[4] I. H. Yılmaz and A. Mwesigye, Modeling, simulation and performance analysis of parabolic trough solar collectors: A comprehensive review, *Applied Energy*, 225 (2018) 135-174.
[5] K. D. Ramesh and K. Suresh, Thermal performance of parabolic trough collector with absorber tube misalignment and slope error, *Solar Energy,* 184 (2019) 249-259.
[6] G. K. Manikandan et al., Enhancing the optical and thermal efficiency of a parabolic trough collector-A review, *Applied Energy*, 235 (2019) 1524-1540.
[7] K. M. Shirvan et al., Numerical study of surface radiation and combined natural convection heat transfer in a solar cavity receiver, *International Journal of Numerical Methods for Heat and Fluid Flow*, 27 (10) (2017) 2385-2399.
[8] D. Mills, Advanced in solar thermal electricity technology, *Solar Energy*, 76 (2004) 19-31.
[9] M. A. Moghimi, K. J. Craig and J. P. Meyer, Optimization of a trapezoidal cavity absorber for the linear Fresnel reflector, *Solar Energy,* 119 (2015) 343-361.
[10] G. Zhu, T. Wendelin, M. J. Wagner and C. Kutscher, History, current state, and future of linear Fresnel concentrating solar collectors, *Solar Energy,* 103 (2014) 639-652.
[11] M. Montes et al., Performance model and thermal comparison of different alternatives for the Fresnel single-tube receiver, *Applied Thermal Engineering,* 104 (2016) 162-175.
[12] E. Bellos et al., Experimental and numerical investigation of a linear Fresnel solar collector with flat plate receiver, *Energy Conversion and Management*, 130 (2016) 44-59.
[13] G. Morin et al., Comparison of linear Fresnel and parabolic trough collector power plants, *Solar Energy,* 86 (2012) 1-12.
[14] P. L. Singh, R. M. Sarviya and J. L. Bhagoria, Thermal performance of linear Fresnel reflecting solar concentrator with trapezoidal cavity absorbers, *Applied Energy,* 87 (2010) 541-550.
[15] Z. Yanqing et al., Design and experimental investigation of a stretched parabolic linear Fresnel reflector collecting system, *Energy Conversion and Management*, 126 (2016) 89-98.
[16] E. Bellos et al., Experimental investigation of the daily performance of an integrated linear Fresnel reflector system, *Solar Energy,* 167 (2018) 220-230.
[17] Z. Hongfei et al., Design and experimental analysis of a cylindrical compound Fresnel solar concentrator, *Solar Energy,* 107 (2014) 26-37.
[18] A. Rawani, S. P. Sharma, K. D. P. Singh and K. Namarata, Analytical modeling of parabolic linear collectors for solar power plant, *Journal of Mechanical Science and Technology*, 32 (10) (2018) 4993-5004.
[19] W. T. Xie, Y. J. Dai and R. Z. Wang, Thermal performance analysis of a line-focus Fresnel lens solar collector using different cavity receivers, *Solar Energy*, 91 (2013) 242-255.
[20] J. C. Duran and R. O. Nicolas, Development and applications of a two-dimensional optical analysis of non-perfect cylindrical concentrators, *Solar Energy*, 34 (1985) 257-269.
[21] H. B. Kulkarni, Design and development of prototype cylindrical parabolic solar collector for water heating application, *Internaional Journal of Renewable Energy Development* (2016) 49-55.
[22] B. Sadhana, L. S. V. Prasad and G. Satyanand, Design aspects of cylindrical parabolic concentrator for sterilization, *International Journal of Emerging Technology and Advanced Engineering,* 4 (8) (2014) 203-209.
[23] P. Math, N. Rao and R. Parasat, Experimental analysis of cylindrical parabolic collector with and without tracking system, *International Journal of Ignited Minds*, 11 (2014) 1-6.
[24] F. Ullah and K. Min, Performance evaluation of dual-axis tracking system of parabolic trough solar collector, *Materials Science and Engineering* (2018) 301-310.
[25] J .A Duffie and W. A. Beckman, *Solar Energy Thermal Processes*, John Wiley and Sons, New York (1991).
[26] A. Kılıç, Solar Energy, Kipaş Distributorship (1984).
[27] F. P. Incropera and D. P. DeWitt, *Heat and Mass Transfer*, Literatür Publishing (translation), Istanbul (2001).
[28] S. Conrado, A. Rodriguez and G. Calderon, Thermal performance of parabolic trough solar collectors, *Renewable and Sustainable Energy Reviews,* 67 (2017) 1345-1359.
[29] J. S. Hesieh, *Solar Energy Engineering*, Prentice-Hall (1986).
[30] C. Çetiner, F. Halıcı and H. Çaçur, The experimental and theoretical investigation on of superheated water in twin-cylindrical solar parabolic collectors, *Isı Bilimive Teknigi Dergisi/Journal of Thermal Science and Technology*, 31 (2011) 87-94.
[31] J. K. Nayak, E. Y. Amer and S. M. Deshpande, Comparison of three transient methods for testing solar flat-plate collector, *Energy Conversions & Nanagement*, 4 (2000) 677-700.
[32] S. M. Jeter, Analytical determination of the optical performance of practical parabolic trough collectors from design data, *Solar Energy*, 39 (1987) 11-21.
[33] E. H. Amer, J. K Nayak and G. K. Sarma, Transient test method for plat-plate collector: review and experimental evaluation, *Solar Energy*, 60 (5) (1997) 229-243.
[34] W. Chamsa et al., Thermal performance testing of heat pipe evacuated tube with compound parabolic concentrating, Solar Collector by ISO 9806 -1, *Energy Procedia*, 56 (2014) 237-246.
[35] H. Beltagy, D. Semmar, C. Lehaut and N. Said, Theoretical and experimental performance analysis of a Fresnel type solar concentrator, *Renewable Energy*, 101 (2017) 782-793.

Cuma Çetiner finished his Ph.D. degree in Sakarya University in Turkey. He has works as an assistant professor at Harran University. His research interest includes solar and renewable energy.